

High Microwave Absorption of Multi-Walled Carbon Nanotubes (Outer Diameter 10 – 20 nm)-Epoxy Composites in R-Band

Abstract

We studied the microwave absorption of multi-walled carbon nanotubes (MWCNTs)-epoxy composites over a continuous frequency range in R-band (26.5 – 40 GHz). The outer diameters (OD) of the MWCNTs were in the 10 – 20 nm range. We measured and analyzed the microstructures, dielectric and the microwave absorption properties of the composite samples. High attenuation factor which correlates significant absorption of microwave was observed in the 32 – 40 GHz frequency band. Microwave absorption was due to high dielectric losses, interfacial charge polarization, and the free electron mobility in the composite material. Our results also show the dependence of microwave absorption on the loading fractions of MWCNTs and on the thickness of the absorbing material. Significant microwave absorption capabilities of the composite samples were achieved at 7 to 10 wt.% of MWCNT loadings for frequencies above 32 GHz.

Keywords: Composites; Nanotubes; Dielectric properties; Conducting polymers; Microwave absorption.

1. Introduction

The combination of structure, topology, and dimensions creates an unparalleled host of physical properties in carbon nanotubes (CNTs) for explorations [1]. These tiny, quasi one-dimensional materials show great promise for a variety of application areas, such as molecular reinforcements in composites, displays, sensors, energy-storage media and molecular electronic devices [2-4].

Multi-walled carbon nanotubes (MWCNTs) are made by rolling a stacking of multiple layers of graphene sheets so as to obtain concentric nanotubes. Like polymer chains in epoxy used as a composite matrix, MWCNTs have practically one-dimension and are flexible. Many exciting and unique properties have been demonstrated for polymers filled with C-based materials, including improved strength and durability, electrical conductivity, flame resistance, UV absorption, and reduced permeability [5-9]. In addition to these properties, the rapid progress in the fabrication of CNTs and large area ($\approx 1 \text{ cm}^2$) graphene flakes [10] make these C structures promising for microwave absorption (MA) applications, e.g., as shielding materials for the protection of electronic devices, reduction in electromagnetic exposure, and others [11]. It has been reported that nanoparticles could provide better absorption properties in the polymer matrix than micro-sized ones; hence, nanocomposite materials could be used successfully as microwave absorbers [12].

Recent studies show that carbon filled polymer matrices can be used for electromagnetic (EM) absorption and interference shielding applications [13-18]. These include reducing electromagnetic interference among electronic components. Other areas of applications include consumer electronics, wireless LAN devices, radar absorbers, wireless antenna system, cellular phones, and others.

Ghasemi et al. [19] reported that the reflection loss of nanocomposites from MWCNTs at the frequency range of 2–18 GHz were better when compared to that of strontium ferrite nanoparticles. They showed that reflection loss improved significantly with an increase in volume percentage of MWCNTs, thus indicating their potential as wide-band electromagnetic wave absorbers. Sutradhar et al. [20] demonstrated from their studies that microwave absorption of nanoparticles of Cu^{2+} doped with Li–Zn ferrite in a frequency of 8 – 18 GHz was drastically enhanced after encapsulation with a non-magnetic matrix of multi-walled carbon nanotubes (MWCNT). The microwave absorption properties of polymer composites can be tailored through changes in geometry, composition, morphology, and fractions of the filler particles [11]. We fabricated MWCNTs-epoxy composites by varying the loading fractions of MWCNTs in epoxy matrix in the range of 1 – 10 wt.%. The diameters of CNTs have a strong influence on their functionality and applications. In this work, the selected outer diameters (OD) of MWCNTs are in the range of 10 – 20 nm. We studied the dielectric and microwave absorption properties of the fabricated CNT-epoxy composites over a continuous frequency range in R-band (26.5 – 40 GHz). Our motivation for this work is to

investigate microwave absorption properties of MWCNT-epoxy composites in R-band when the loading fraction of MWCNTs increases in the matrix, given that relatively lower frequencies (< 20 GHz) have been well studied. The matrix used in fabricating these nanocomposites is the epoxy resin. Epoxy resin or polyepoxide is a thermosetting polymer that cures when mixed with a catalyzing agent or hardener. It is known for its excellent adhesion as well as chemical and heat resistance. It also has excellent mechanical strength and good electrical insulating properties, thereby making it a good candidate as a polymer matrix material when MWCNTs are dispersed in it.

2. Experiments

2.1 Materials

The MWCNTs were obtained from Cheap Tubes Inc. USA. Epoxy Resin #300 and Hardener #11 were purchased from Aeromarine Products Inc. USA. The outer diameters (OD) of the MWCNTs are in the range of 10 – 20 nm; their length distribution is within the range of 10 – 30 μm . The purity content of MWCNTs in the powder form is greater than 95 wt.%, while the ash content is less than 1.5 wt.%.

2.2 Sample Fabrication

A mechanical mixture method was employed in the fabrication of the MWCNTs–epoxy composites. The MWCNTs with loading fractions of 1-10 wt.% were mixed in epoxy using a hot plate magnetic stirring machine for 1 hour at 120 rpm and 90°C. The procedure ensures proper dispersion of MWCNTs in the epoxy resin by reducing its viscosity and eliminating the formation of air bubbles in the mixture during stirring. The highest MWCNT loading in the epoxy matrix was 10 wt.%, beyond which a uniform sample could not be fabricated. Aeromarine hardener was then added with the same mass ratio as the epoxy resin and stirred carefully for about 10 minutes for pre-curing. Release Agent (PTFE: Miller Stephenson, MS-122AD) was sprayed onto the sample molds and allowed to dry for 10 minutes. This action is to aid the removal of sample from the molds after curing. The mixture was then infused into waveguide molds of varying dimensions and placed in the oven for post-curing at 80°C for 1 hour. The waveguide molds produce two composite sample sizes of 2 mm and 3 mm thickness (length 7.1 mm and width 3.5 mm) after post-curing. The composite sample sizes were dictated by the sample hold of the measurement instrument.

2.3 Instruments and Measurements

An Agilent N5230C PNA-L Microwave Network Analyzer (Agilent Company, USA) was used to measure the scattering parameters (s – parameters). Measurements were taken at room temperature. The relative complex dielectric permittivity $\varepsilon = \varepsilon' - j\varepsilon''$ was also measured by the PNA-L Network Analyzer using the Agilent Technology 85071E Material measurement software for the R-band frequency range of 26.5 – 40 GHz for all the samples.

The scanning electron microscopy (SEM) images of some selected samples were obtained using Hitachi S-4500 II (Japan) with an accelerated voltage of 10 KV. Gold sputtering was first performed on all the samples for improved conductivity before taking the SEM images. X-Ray Diffraction (XRD) technique was used to characterize the microstructures of the samples using the Rigaku MiniFlex 600 XRD instrument. The MiniFlex XRD instrument has an X-ray tube voltage of 40 kV, wavelength, λ for a Copper X-ray source of 1.5406 Å and 2θ scanning range from 10° to 80°.

3. Results and Discussion

3.1 Morphological Characterization using SEM

The structural morphology of selected MWCNTs-epoxy composites with different MWCNTs loadings were examined using SEM, as shown in Fig. 1. Due to the weak van der Waals' interaction force between the individual carbon tubes, the MWCNTs in the samples formed MWCNT bundles. The MWCNT bundles are sparsely dispersed in the epoxy resin at 2 wt.% MWCNT loading [Fig. 1(a)]. The MWCNT bundles become more visible in the composite as the MWCNT loading fraction increases to 9 wt.% in epoxy [Fig. 1(b)]. The SEM image of the

composite sample with 9 wt.% MWCNTs loading depicts a dense, and well dispersed MWCNTs (tiny white bundles) in the composite.

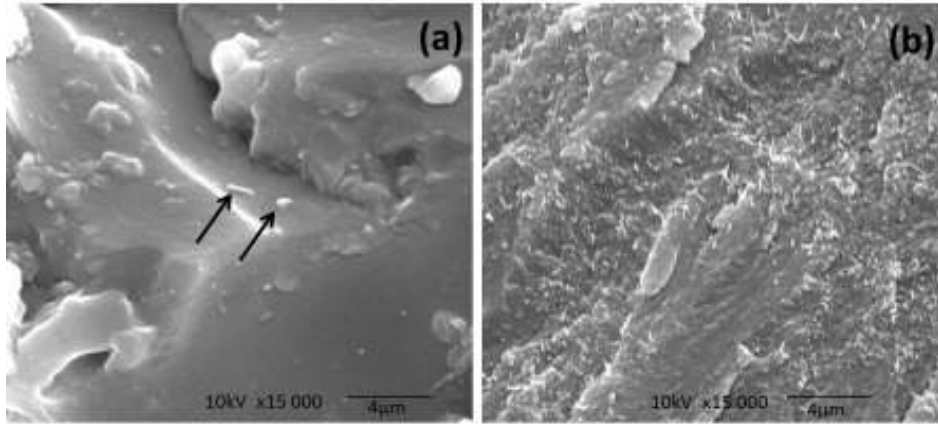


Figure 1. SEM images of MWCNT-epoxy composite samples with the MWCNT loading of (a) 2 wt.% and (b) 9 wt.%. The black arrows in (a) points to dispersed MWCNTs in the epoxy matrix. MWCNTs are much more numerous and visible (everywhere) in the 9 wt.% sample as compared to the 2 wt.% one.

3.2 X-Ray Diffraction Measurement

Table 1 and Figure 2 show the analytical data and patterns of the X-ray diffraction (XRD) of the pure epoxy and MWCNTs-epoxy composites, respectively. The sharp narrow reflection peak at $2\theta = 26.14^\circ$ of the MWCNTs conforms to the interlayer distance (002) between the multi-walled carbon nanotubes. This interlayer distance is approximately 3.40 \AA , and it is comparable to the distance between graphene layers in graphite. The weak reflection peak (100) of the pure MWCNTs at $2\theta = 43.48^\circ$ implies a characteristic of turbostratic graphite lacking interlayer stacking correlation [21]. The characteristic peaks of the MWCNTs are visible in the XRD of the MWCNT-epoxy composites (Fig. 2). Specifically, the weak peak structures at $2\theta = 25.72^\circ$, indicates that MWCNTs retained their structural characteristics in the composites.

The reflection peak at $2\theta = 19.06^\circ$ was observed for the pure epoxy sample. The major reflection peak positions at $2\theta = 19.06^\circ$ in the epoxy composites with 2, 5, 7 and 9 wt.% of MWCNTs were observed to align with that of pure epoxy, signifying the preservation of the microstructures of the epoxy and MWCNTs. The peak shape around $2\theta = 19.06^\circ$ changes slightly, including the peak width and the appearance of a shoulder structure at $2\theta = 25.72^\circ$, as the loading fraction of MWCNTs increases in epoxy, indicating a weak van der Waals' interaction between the epoxy resin and MWCNTs.

Samples	Peak 1			Peak 2		
	$2\theta (^\circ)$	Peak Value (a.u.)	Peak Width ($^\circ$)	$2\theta (^\circ)$	Peak Value (a.u.)	Peak Width ($^\circ$)
MWCNTs	26.14	1909.16	3.94	43.48	344.54	2.56
Pure Epoxy	19.06	1472.29	9.10	-	-	-
2 wt.%MWCNTs	19.06	1363.95	7.22	25.72	615.05	-
5 wt.%MWCNTs	19.06	1337.14	7.18	25.72	643.44	-
7 wt.%MWCNTs	19.06	1321.58	6.16	25.72	665.16	-
9 wt.%MWCNTs	19.06	1312.02	6.76	25.72	617.32	-

Table 1. Analytical data (peak position, peak value, and peak width) from XRD measurements for MWCNTs, pure epoxy, and MWCNTs-epoxy composites (see Fig. 2). Two major peaks (1 and 2) are presented in the table for the samples. Blank cells in the table (marked by a minus sign) are 2θ positions where peak structure is either absent or not very prominent.

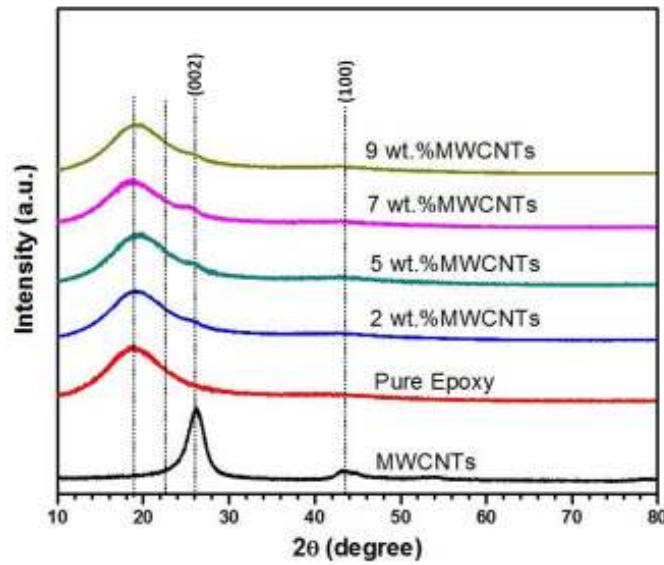


Figure 2. XRD patterns of MWCNTs, pure epoxy, and MWCNTs-epoxy composites.

3.3 Complex Dielectric Permittivity.

According to the transmission line theory [22], when an electromagnetic wave is transmitted through a material, the reflectivity and absorption are affected by factors such as permittivity, permeability, frequency, and the thickness of the material or absorber. These factors may cause either dielectric or magnetic loss in the material. In this work, we measured the dielectric permittivity (real and imaginary part) of the pure epoxy and MWCNTs-epoxy composites in the frequency range 26.5 – 40 GHz. The measurement data show that real part of the relative magnetic permeability μ is about 1.0 and the imaginary part of the relative permeability is nearly 0.0, within the measurement uncertainty of about $\pm 5\%$, because our samples are non-magnetic.

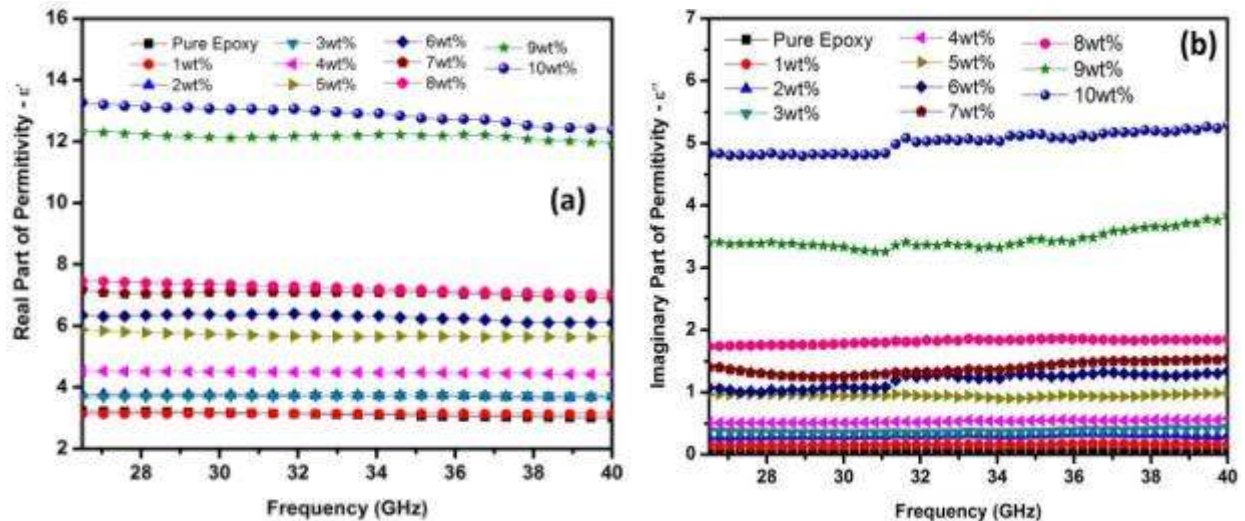


Figure 3. Real part (ϵ') and Imaginary part (ϵ'') of relative dielectric permittivity of pure epoxy and MWCNTs-epoxy composites with MWCNT loading fractions from 1 – 10 wt.%.

The measurement results showed the dependence of real part ϵ' and imaginary part ϵ'' of permittivity on the loading fractions of MWCNTs in the composites as shown in Fig. 3 [23-26]. The values of ϵ' and ϵ'' increase as the

loading fraction of MWCNTs increases. Substantial increases in ϵ' and ϵ'' were observed for composite samples (sample thickness is 3 mm) with 9 and 10 wt.% MWCNT loading fractions [Fig 3 (a) and (b)]. The real part of the permittivity, ϵ' , is related to a measure of the energy storage capability in the material from electromagnetic field [11]. Figure 3 (b) shows the dependence of the imaginary part of permittivity, ϵ'' on frequency. The imaginary part of permittivity, ϵ'' indicates the dissipative tendency of a material to electromagnetic fields, and it is related to its microwave absorption capabilities. We noticed a substantial increase in the values of ϵ'' for the samples with 9 and 10 wt.% MWCNT loadings [Fig 3 (b)]. As the loading fraction increases, conductive charges from the MWCNTs enhance the charge polarizations between MWCNTs (CNT aggregates) and epoxy matrix. The conductive electrons and charge polarizations becomes more effective in interacting with the microwave field thereby enhancing the microwave absorption properties of the material [25]. The high values of ϵ'' in the 9 and 10 wt.% MWCNTs in the composites signify high dielectric absorption of external EM wave by the material, resulting from increased loadings of MWCNTs. The real part of the permittivity, ϵ' for the same samples decreases [Fig 3(a)] as the frequency increases. These phenomena of decreasing values of ϵ' versus increasing ϵ'' as the frequency increases, are understood in terms of the correlation between ϵ' and ϵ'' for the fact that the displacement current significantly lags behind the built-up potential across the sample as the electromagnetic wave frequency increases [25]. Our results showed that increasing the loading fractions of MWCNTs in the composites influences the values of ϵ' and ϵ'' which as we have seen, enhances the microwave absorption of the composite sample.

3.4 Dielectric Loss Tangent

The dielectric loss tangent of a material is a ratio of the imaginary part ϵ'' to the real part ϵ' of the permittivity. This quantity is a measure of loss in a material for a given sample thickness at a specified wavelength. It determines the attenuating factor of the material [26]. Increasing loss tangent shows improved attenuating properties in the material. Our results show that increasing the loading fraction of MWCNTs in the matrices enhances the loss tangents of the composite samples [Fig 4]. The MWCNTs-epoxy composite with 10 wt.% MWCNT loading has high loss performance; the loss tangent for the sample is 0.37 for frequencies less than 31 GHz, but gradually increases up to 0.42 for frequencies in 32 – 40 GHz range. The significant increase in the loss tangent of the composite with 10 wt.% MWCNT loading contributes to higher EM attenuation factor in the 32 – 40 GHz range.

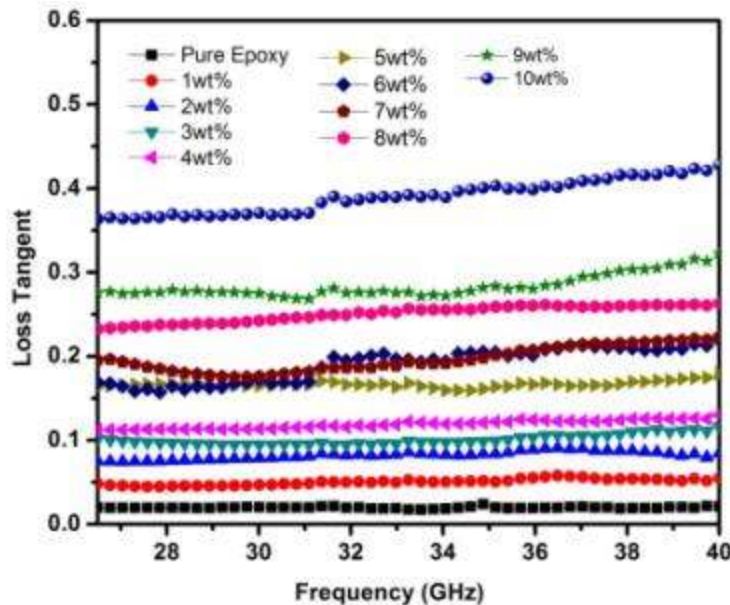


Figure 4. Dielectric loss tangents of pure epoxy and MWCNTs-epoxy samples with MWCNT loading fractions from 1 – 10 wt.%.

3.5. Microwave Absorption in the MWCNT-Epoxy Composites

When a microwave beam is incident on a material, some of its energy is reflected, absorbed, or transmitted. The transmission and reflection losses of microwave in absorbing material play an important role in applications. The transmission and reflection loss are obtained from the scattering parameters (s-parameters). We used the Agilent N5230C PNA-L Microwave Network Analyzer to measure the scattering parameters. The transmittance (T), reflectance (R), and absorbance (A) through the composite material can be described as below [27]:

$$T = |S_{21}|^2 (= |S_{12}|^2) \quad (1)$$

$$R = |S_{11}|^2 (= |S_{22}|^2) \quad (2)$$

$$A = 1 - R - T \quad (3)$$

where S_{11} (or S_{22}) and S_{21} (or S_{12}) are the reflection and transmission coefficients, respectively. The absorbance A , also referred to as the absorption ratio, is a measure of the microwave absorption capability of the material under test. The transmission and reflection loss of the fabricated MWCNTs-epoxy composite samples were measured over a continuous frequency range in R-band (26.5-40 GHz).

The frequency dependence of reflection loss (RL) can also be evaluated from the complex permittivity ($\epsilon_r = \epsilon'_r - j\epsilon''_r$) and permeability ($\mu_r = \mu'_r - j\mu''_r$) according to the following equations [22]

$$Z_{in} = Z_0 \left(\frac{\mu_r}{\epsilon_r} \right)^{1/2} \tanh \left[j \left(\frac{2\pi f d}{c} \right) \mu_r \epsilon_r^{1/2} \right] \quad (4)$$

$$RL = 20 \log \left| \frac{Z_{in} - Z_0}{Z_{in} + Z_0} \right| \quad (5)$$

where f is the microwave frequency; d is the thickness of the absorber (in this case the CNT-epoxy composite samples); Z_0 is the impedance of air; Z_{in} is the input impedance of the absorber; and c is the speed of light in the vacuum.

The absorption ratio (in %) versus microwave frequency (GHz) for the 2 mm and 3 mm composite samples is shown in Fig. 5 (a) and (b).

Clearly, the pure epoxy samples (both 2 and 3 mm thicknesses) have very low microwave absorption capability. Our results show that the microwave absorption in composite materials strongly depends on the loading fraction of MWCNTs in epoxy. Increase in the loading fraction of MWCNTs in epoxy substantially increases the microwave absorption. The effect of the sample thickness on the microwave absorption of the composites was observed in lower loadings of MWCNTs for frequencies lower than 34 GHz. The 3 mm composite samples (with 1 – 5 wt.% MWCNTs) have higher absorption ratios in the lower frequencies (below 34 GHz) than those of the 2 mm sample as showed in Fig. 5. For higher MWCNT loading fractions (i.e. 6 – 10 wt.%), the microwave absorption ratios of the samples becomes complex as showed in Fig. 5 (a) and (b). This complexity is attributed to the high dielectric loss and free electron mobility in MWCNTs-epoxy composites.

The dispersion of MWCNTs in epoxy clearly enhances the microwave absorption properties of the composite. The defects in the MWCNT-epoxy composites also influence the reflection loss and absorption properties of the samples. In particular, defects could affect the morphology and functionality of the MWCNTs-epoxy composites. Porous structures could contribute to microwave absorption properties [28-31]. Multiple reflections and scattering occur when microwave is incident on a porous structure, causing loss of electromagnetic energy [32]. Defects such as stacking faults, grain boundaries and interfaces, which can cause charge polarization and relaxation, are reported to improve microwave absorption [33-35]. It is difficult to identify accurately and quantitatively the type of defects contained in composite materials, and there is no known standards to distinguish them systematically [36]. The formation of MWCNT aggregates [37] and active electrons [38] in the composites with higher MWCNT loading have been suggested as possible mechanisms responsible for the complexities in their microwave absorption properties. As we increase the concentration of MWCNTs in the matrix, it reaches and eventually surpasses the percolation threshold of the composite samples, thus impacting significantly on its effective dielectric and microwave absorption characteristics [11]. Once the percolation threshold is exceeded, a phase

transition from an insulating to a conducting state occurs in the composite sample which also influences microwave absorption [39]. The 2 mm composite sample with 7 wt.% MWCNTs has a steady absorption performance over a broad frequency band as shown in Fig. 5(a). Especially, the 2 mm composite sample with 7 wt.% MWCNTs shows quite high (45 to 60 %) microwave absorption in a wide frequency band (from 26.5 to 40 GHz). From these results, optimum loading fractions of the MWCNTs was achieved at 7 wt.%. Further increases in the loading fractions of the MWCNTs in epoxy did not significantly affect the microwave absorption capabilities of the composite samples as shown in Fig. 5 (a). The 2 mm samples with 7, 8 and 9 wt.% MWCNTs can be used as microwave absorbers in applications where a steady absorption performance is required.

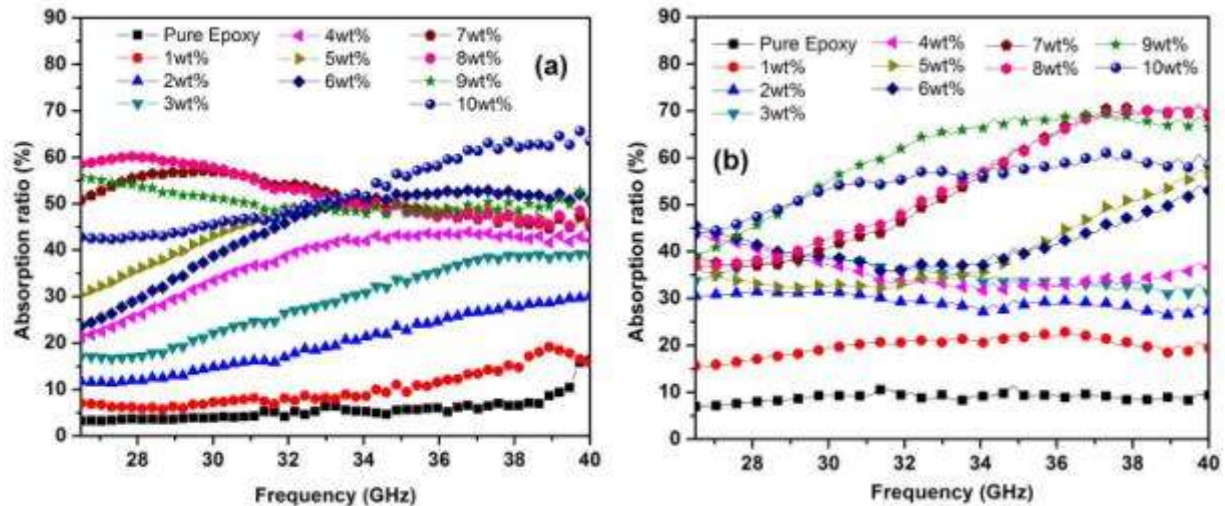


Figure 5. Absorption ratio (in %) of (a) 2 mm and (b) 3 mm pure epoxy and MWCNTs-epoxy samples with MWCNT loading fractions from 1 – 10 wt.%.

The microwave absorption ratio of the 3 mm MWCNTs-epoxy samples with higher MWCNT loadings (7, 8, 9, and 10 wt.%) increases as the microwave frequency increases [Fig. 5(b)]. The 3 mm MWCNTs-epoxy samples with 7 and 8 wt.% MWCNTs produce high absorption ratio (about 70%) in a narrow frequency range 37 – 40 GHz. The 3 mm composite sample with 9 wt.% MWCNTs shows a steady microwave absorption ratio (45 to 67 %) over a wider frequency range (29 – 40 GHz). Increasing the MWCNT loading to 10 wt.%, for the 3 mm composite sample, a lower microwave absorption was observed.

For both (2 and 3 mm) composite samples, the maximum steady absorption ratio of the microwave radiation was around 60 – 67 %, showing weak dependence on the thickness of the absorber, especially at higher loading fractions of MWCNTs in the composites.

Since MWCNTs are nonmagnetic materials, their microwave absorption mainly originates either from polarization, ohmic losses, or multiple scattering. For the MWCNTs-epoxy composites, the presence of large amount of interfaces between the high aspect ratio of MWCNTs and epoxy matrix benefit the improvement of interfacial charge polarization. External electromagnetic radiation can be attenuated due to the interaction of microwave energy with charge multipoles at polarized interfaces. This will contribute to the absorption of electromagnetic energy. Interface scattering due to the difference in the effective permittivity between conductive MWCNTs and insulating epoxy host can also contribute to the microwave absorption in the composites. In addition, the free electric charges from the electrically conductive MWCNTs with relatively high MWCNT loadings in the epoxy composite will interact with electromagnetic wave, dissipate the radiation energy to heat, and contribute to the absorption of electromagnetic energy.

4. Conclusion

In this work, MWCNTs-epoxy composites were fabricated using MWCNTs (outer diameter of 10 – 20 nm) with loading fraction ranging from 1 to 10 wt.%. We studied the microstructure, dielectric permittivity, and microwave absorption properties of the composites within the frequency range of R-band (26.5 – 40 GHz). The 3 mm

MWCNTs-epoxy samples with 7 and 8 wt.% MWCNTs show high absorption ratio (about 70 %) in a narrow frequency range of 37 – 40 GHz. The 3 mm composite sample with 9 wt.% MWCNTs shows steady microwave absorption ratio (45 to 67 %) over a wider frequency range (29 – 40 GHz), an indication of potential applications for steady microwave absorption. The microwave absorption of the samples is due to high dielectric loss, interfacial charge polarization, and free electron mobility of MWCNTs. Our result (high microwave absorption ratio up to 70 %) suggest that this group of MWCNTs (OD: 10 -20 nm), has potentials for high, as well as for broad bandwidth microwave absorption applications.

Acknowledgment

This research work is funded in part by the US Air Force Office of Scientific Research (Award No FA9550-09-1-0367 and FA9550-11-1-0330), the US National Science Foundation (NSF) and the Louisiana Board of Regents, through LASiGMA project [Award Nos. EPS-1003897, NSF (2010-15)-RII-SUBR].

References

1. Endo, M., M. Strano, and P. Ajayan, *Potential Applications of Carbon Nanotubes*, in *Carbon Nanotubes*, A. Jorio, G. Dresselhaus, and M. Dresselhaus, Editors. 2008, Springer Berlin Heidelberg. p. 13-62.
2. Baughman, R.H., A.A. Zakhidov, and W.A. de Heer, *Carbon Nanotubes--the Route Toward Applications*. Science, 2002. **297**(5582): p. 787-792.
3. Ajayan, P.M., *Nanotubes from Carbon*. Chemical Reviews, 1999. **99**(7): p. 1787-1800.
4. Boris Yakobson, R.S., *Fullerene Nanotubes: C1,000,000 and Beyond*. American Scientist, 1997. **85**: p. 324.
5. Qian, D., G.J. Wagner, W.K. Liu, M.-F. Yu, and R.S. Ruoff, *Mechanics of carbon nanotubes*. Applied Mechanics Reviews, 2002. **55**(6): p. 495-533.
6. Kim, H.M., K. Kim, C.Y. Lee, J. Joo, S.J. Cho, H.S. Yoon, D.A. Pejaković, J.W. Yoo, and A.J. Epstein, *Electrical conductivity and electromagnetic interference shielding of multiwalled carbon nanotube composites containing Fe catalyst*. Applied Physics Letters, 2004. **84**(4): p. 589-591.
7. Yang, Y., M.C. Gupta, K.L. Dudley, and R.W. Lawrence, *Conductive Carbon Nanofiber-Polymer Foam Structures*. Advanced Materials, 2005. **17**(16): p. 1999-2003.
8. Zhang, X.F., X.L. Dong, H. Huang, Y.Y. Liu, W.N. Wang, X.G. Zhu, B. Lv, J.P. Lei, and C.G. Lee, *Microwave absorption properties of the carbon-coated nickel nanocapsules*. Applied Physics Letters, 2006. **89**(5): p. 053115.
9. Che, R.C., L.M. Peng, X.F. Duan, Q. Chen, and X.L. Liang, *Microwave Absorption Enhancement and Complex Permittivity and Permeability of Fe Encapsulated within Carbon Nanotubes*. Advanced Materials, 2004. **16**(5): p. 401-405.
10. Li, X., W. Cai, J. An, S. Kim, J. Nah, D. Yang, R. Piner, A. Velamakanni, I. Jung, E. Tutuc, S.K. Banerjee, L. Colombo, and R.S. Ruoff, *Large-Area Synthesis of High-Quality and Uniform Graphene Films on Copper Foils*. Science, 2009. **324**(5932): p. 1312-1314.
11. Qin, F. and C. Brosseau, *A review and analysis of microwave absorption in polymer composites filled with carbonaceous particles*. Journal of Applied Physics, 2012. **111**(6): p. 061301.
12. Micheli, D., C. Apollo, R. Pastore, and M. Marchetti, *X-Band microwave characterization of carbon-based nanocomposite material, absorption capability comparison and RAS design simulation*. Composites Science and Technology, 2010. **70**(2): p. 400-409.
13. Ye, Z., Z. Li, J.A. Roberts, P. Zhang, J.T. Wang, and G.L. Zhao, *Electromagnetic wave absorption properties of carbon nanotubes-epoxy composites at microwave frequencies*. Journal of Applied Physics, 2010. **108**(5): p. 054315.
14. Ren, F., H. Yu, L. Wang, M. Saleem, Z. Tian, and P. Ren, *Current progress on the modification of carbon nanotubes and their application in electromagnetic wave absorption*. RSC Advances, 2014. **4**(28): p. 14419-14431.
15. Pawar, S.P., D.A. Marathe, K. Pattabhi, and S. Bose, *Electromagnetic interference shielding through MWNT grafted Fe₃O₄ nanoparticles in PC/SAN blends*. Journal of Materials Chemistry A, 2015. **3**(2): p. 656-669.
16. Wang, Z. and G.-L. Zhao, *Electromagnetic wave absorption of multi-walled carbon nanotube-epoxy composites in the R band*. Journal of Materials Chemistry C, 2014. **2**(44): p. 9406-9411.

- 330 17. Zou, T., H. Li, N. Zhao, and C. Shi, *Electromagnetic and microwave absorbing properties of multi-walled*
331 *carbon nanotubes filled with Ni nanowire*. Journal of Alloys and Compounds, 2010. **496**(1–2): p. L22-L24.
- 332 18. Wen, F., F. Zhang, J. Xiang, W. Hu, S. Yuan, and Z. Liu, *Microwave absorption properties of multiwalled*
333 *carbon nanotube/FeNi nanopowders as light-weight microwave absorbers*. Journal of Magnetism and
334 Magnetic Materials, 2013. **343**(0): p. 281-285.
- 335 19. Ghasemi, A., S.E. Shirsath, X. Liu, and A. Morisako, *A comparison between magnetic and reflection loss*
336 *characteristics of substituted strontium ferrite and nanocomposites of ferrite/carbon nanotubes*. Journal
337 of Applied Physics, 2012. **111**(7): p. 07B543.
- 338 20. Sutradhar, S., S. Das, and P.K. Chakrabarti, *Magnetic and enhanced microwave absorption properties of*
339 *nanoparticles of $\text{Li}_{0.32}\text{Zn}_{0.26}\text{Cu}_{0.1}\text{Fe}_{2.32}\text{O}_4$ encapsulated in carbon nanotubes*. Materials Letters, 2013.
340 **95**(0): p. 145-148.
- 341 21. Warren, B.E., *X-Ray Diffraction in Random Layer Lattices*. Physical Review, 1941. **59**(9): p. 693-698.
- 342 22. Michielssen, E., J.M. Sajer, S. Ranjithan, and R. Mittra, *Design of lightweight, broad-band microwave*
343 *absorbers using genetic algorithms*. Microwave Theory and Techniques, IEEE Transactions on, 1993. **41**(6):
344 p. 1024-1031.
- 345 23. Xiang, C., Y. Pan, X. Liu, X. Sun, X. Shi, and J. Guo, *Microwave attenuation of multiwalled carbon nanotube-*
346 *fused silica composites*. Applied Physics Letters, 2005. **87**(12): p. 123103.
- 347 24. Wu, J. and L. Kong, *High microwave permittivity of multiwalled carbon nanotube composites*. Applied
348 Physics Letters, 2004. **84**(24): p. 4956-4958.
- 349 25. Watts, P.C.P., D.R. Ponnampalam, W.K. Hsu, A. Barnes, and B. Chambers, *The complex permittivity of*
350 *multi-walled carbon nanotube-polystyrene composite films in X-band*. Chemical Physics Letters, 2003.
351 **378**(5–6): p. 609-614.
- 352 26. Hippel, A.R.V., *Dielectrics and Waves*. 527-24. 1995, New York: Artech House Print.
- 353 27. Saini, P., V. Choudhary, B.P. Singh, R.B. Mathur, and S.K. Dhawan, *Polyaniline–MWCNT nanocomposites*
354 *for microwave absorption and EMI shielding*. Materials Chemistry and Physics, 2009. **113**(2–3): p. 919-926.
- 355 28. Liu, Q., D. Zhang, and T. Fan, *Electromagnetic wave absorption properties of porous carbon/Co*
356 *nanocomposites*. Applied Physics Letters, 2008. **93**(1): p. 013110-013113.
- 357 29. Zhou, J., J. He, G. Li, T. Wang, D. Sun, X. Ding, J. Zhao, and S. Wu, *Direct Incorporation of Magnetic*
358 *Constituents within Ordered Mesoporous Carbon–Silica Nanocomposites for Highly Efficient*
359 *Electromagnetic Wave Absorbers*. The Journal of Physical Chemistry C, 2010. **114**(17): p. 7611-7617.
- 360 30. Chen, Y.-J., P. Gao, R.-X. Wang, C.-L. Zhu, L.-J. Wang, M.-S. Cao, and H.-B. Jin, *Porous $\text{Fe}_3\text{O}_4/\text{SnO}_2$*
361 *Core/Shell Nanorods: Synthesis and Electromagnetic Properties*. The Journal of Physical Chemistry C, 2009.
362 **113**(23): p. 10061-10064.
- 363 31. Mu, G., N. Chen, X. Pan, K. Yang, and M. Gu, *Microwave absorption properties of hollow*
364 *microsphere/titania/M-type Ba ferrite nanocomposites*. Applied Physics Letters, 2007. **91**(4): p. 043110.
- 365 32. Zhu, H.-L., Y.-J. Bai, R. Liu, N. Lun, Y.-X. Qi, F.-D. Han, X.-L. Meng, J.-Q. Bi, and R.-H. Fan, *Microwave*
366 *absorption properties of MWCNT-SiC composites synthesized via a low temperature induced reaction*. AIP
367 Advances, 2011. **1**(3): p. 032140.
- 368 33. Meng, B., B.D.B. Klein, J.H. Booske, and R.F. Cooper, *Microwave absorption in insulating dielectric ionic*
369 *crystals including the role of point defects*. Physical Review B, 1996. **53**(19): p. 12777-12785.
- 370 34. Zhang, X.F., X.L. Dong, H. Huang, B. Lv, J.P. Lei, and C.J. Choi, *Microstructure and microwave absorption*
371 *properties of carbon-coated iron nanocapsules*. Journal of Physics D: Applied Physics, 2007. **40**(17): p.
372 5383.
- 373 35. Liu, X.G., D.Y. Geng, H. Meng, P.J. Shang, and Z.D. Zhang, *Microwave-absorption properties of ZnO-coated*
374 *iron nanocapsules*. Applied Physics Letters, 2008. **92**(17): p. 173117.
- 375 36. Lehman, J.H., M. Terrones, E. Mansfield, K.E. Hurst, and V. Meunier, *Evaluating the characteristics of*
376 *multiwall carbon nanotubes*. Carbon, 2011. **49**(8): p. 2581-2602.
- 377 37. Dietrich Stauffer, A.A., *Introduction To Percolation Theory*. Second Edition ed. 1994: CRC Press.
- 378 38. M, R., C.O. Yoon, C.Y. Yang, D. Moses, P. Smith, A.J. Heeger, and Y. Cao, *Transport in polyaniline networks*
379 *near the percolation threshold*. Physical Review B, 1994. **50**(19): p. 13931-13941.
- 380 39. Li, Z., G. Luo, F. Wei, and Y. Huang, *Microstructure of carbon nanotubes/PET conductive composites fibers*
381 *and their properties*. Composites Science and Technology, 2006. **66**(7–8): p. 1022-1029.

